

Two-Way Ranging During Early Mission Phase

Peter W. Kinman
EECS Department
Case Western Reserve University
10900 Euclid Ave
Cleveland, OH 44106-7071
(216) 368-5550
pwk@eecs.cwru.edu

Jeff B. Berner
Mail Stop 238-737
Jet Propulsion Laboratory
4800 Oak Grove Dr.
Pasadena, CA 91109-8099
(818) 354-3934
jeff.b.berner@jpl.nasa.gov

Abstract—The range of a deep space vehicle is commonly measured today using a sequential ranging signal that is transponded at the spacecraft. The noise performance and the uplink spectrum of this scheme are characterized here. In evaluating the performance, emphasis is given to the case of early mission phase, where parameter values are often atypical for the mission as a whole. In particular, during early mission phase, sequential ranging may cause a problem for conical-scan tracking.

TABLE OF CONTENTS

1. INTRODUCTION
 2. SIGNAL MODELS
 3. UPLINK SPECTRUM
 4. TWO-WAY PERFORMANCE
 5. CONSCAN PROBLEM
 6. CONCLUSIONS
- APPENDIX A: JACOBI-ANGER IDENTITIES
APPENDIX B: SQUAREWAVE CHOPPING
APPENDIX C: SINEWAVE CHOPPING
APPENDIX D: NOISE APPROXIMATIONS
REFERENCES

1. INTRODUCTION

In the Deep Space Network (DSN), the range to a distant spacecraft is determined by measuring the time taken by a ranging signal to make one round trip to the spacecraft. The ground tracking station transmits an uplink carrier that has been phase modulated by a ranging signal. The spacecraft transponder demodulates the uplink carrier, filters the ranging signal, and modulates the phase of the downlink carrier with the filtered ranging signal. The downlink carrier is received by a ground tracking station and demodulated. The two-way delay of the ranging signal is determined, and this is a measure of the range.[1,2]

The most common ranging signal in use by the DSN is a sequence of periodic signals.[3] The periodic signals are called range code components. In the original design, the range code components were squarewaves, and the technique was called sequential squarewave ranging. Under the Network Simplification Plan for the DSN, the highest-frequency components are now sinewaves, and the remainder are squarewaves. This change is being made in order to limit the bandwidth of the modulated carrier.

This paper calculates uplink spectrum and two-way performance when ranging with the new ranging sequences. The analysis given here is quite general. Special consideration is given to the feeding through of command signal to the downlink because this can affect performance during early mission phase. Also, the use of sequential ranging signals during early mission phase may sometimes lead to problems for conical-scan (conscan) pointing of the ground antenna.

The paper begins with the definition of mathematical models for the signals. Then equations are given for the spectrum of the uplink carrier when modulated by ranging signal. Then the paper presents an approximate analysis of the two-way ranging performance in the presence of noise. Finally, the problem of conscan tracking while ranging during early mission phase is discussed.

2. SIGNAL MODELS

The highest-frequency component in sequential ranging is called the range clock. Its frequency, which is coherently related to that of the uplink carrier, determines the precision of the range measurement. A typical value for the range clock frequency is 1 MHz. Since a range clock is periodic, any measurement of its time delay will have ambiguity. The purpose of all other components is to resolve that ambiguity. The range clock is the first component sent during a range measurement. Each subsequent component has a frequency equal to one-half that of its immediate predecessor. The sequence continues with components of ever lower frequency, with a halving of the component frequency (a doubling of

¹0-7803-7651-X/03/\$17.00 ©2003 IEEE

²IEEEAC paper #1061

the component period) at each step, until a component is reached whose period is larger than the uncertainty in the *a priori* estimate of two-way delay. For example, if the range clock frequency is 1 MHz, the next component has a frequency of 500 kHz, and this is followed by components with frequencies 250 kHz, 125 kHz, 62.5 kHz, etc. The ratio of the frequency of the range clock to that of any other component is always a power of 2.

Some of the range code components have frequencies that make them potential interferers to the command signal, which shares the uplink with the ranging signal, or to the carrier itself. A simple expedient eliminates this interference problem. As the ranging sequence progresses, with a halving of the component frequency at each step, there comes a point where the component frequency is low enough to be a potential interferer to command or carrier. At this point, a new element is introduced into the signal structure. This new element is a composite signal equal to the product of the current component and a higher-frequency component. Beginning with this component and for each successive component, it is a composite signal of this type, rather than the pure component alone, that modulates the phase of the uplink carrier. This multiplication by a higher-frequency component is called chopping. The higher-frequency component is called the chopping component, and its frequency is called the chopping frequency. The effect of chopping is to shift most of the ranging code sideband power further away from the carrier and the command sidebands, greatly reducing the potential for interference. In the original sequential ranging design, all components were squarewaves, so the chopping component was always a squarewave. Now, however, the chopping component will typically be sinewave.

Figure 1 shows an example chopped range code component. One period T_r of the composite signal, which equals one period of the unchopped component, is shown. In the case shown in this figure, the chopping component is a squarewave, and the chopping frequency is 4 times that of the range code component.

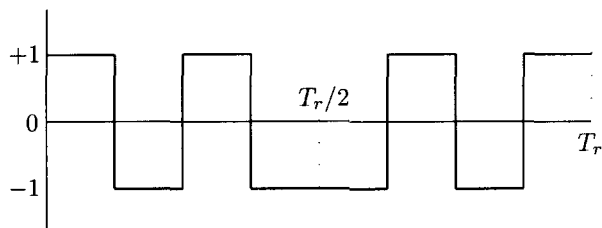


Figure 1: Squarewave chopping: $r(t) = S(\omega_r t) \cdot S(4\omega_r t)$

The uplink carrier is modeled here as a unity-power signal that

is phase modulated by command and ranging signal.

$$s_u(t) = \sqrt{2} \sin \left[\omega_o t + \sqrt{2} \phi_c c(t) \sin \omega_{sc} t + \phi_r r(t) \right] \quad (1)$$

The following symbols are used:

- ω_o = angular frequency of uplink carrier
- ω_{sc} = angular frequency of command subcarrier
- $c(t)$ = command data = ± 1
- $r(t)$ = ranging signal (one of the signals of Table 1)
- ϕ_c = command modulation index, rad rms
- ϕ_r = uplink ranging modulation index, rad rms

Table 1 shows the four possibilities for the ranging signal $r(t)$. (The functions $\alpha(\theta)$ and $\beta(\theta)$ are defined in Section 4, where they are needed for the performance analysis.) The angular frequency ω_r is related to the period T_r of the ranging signal by

$$\omega_r = \frac{2\pi}{T_r}. \quad (2)$$

The first model for $r(t)$ is a squarewave. The symbol $S(\cdot)$ represents a squarewave,

$$S(x) = \text{sgn}[\sin(x)], \quad (3)$$

where the signum function, $\text{sgn}(\cdot)$, is defined by

$$\text{sgn}(x) = \begin{cases} +1, & x \geq 0 \\ -1, & x < 0. \end{cases} \quad (4)$$

The second model for $r(t)$ is a sinewave. The third model is a squarewave chopped (multiplied) by a squarewave. The fourth model is a squarewave chopped by a sinewave. In the latter two models, in which chopping is used, the angular chopping frequency is $m\omega_r$, where m is a power of 2,

$$m = 2^q, \quad q \text{ is from the set } \{1, 2, 3, \dots, 20\}. \quad (5)$$

$r(t)$	$\alpha(\theta)$	$\beta(\theta)$
$S(\omega_r t)$	$\cos \theta$	$\sin \theta$
$\sqrt{2} \sin(\omega_r t)$	$J_0(\sqrt{2}\theta)$	$\sqrt{2}J_1(\sqrt{2}\theta)$
$S(\omega_r t) \cdot S(m\omega_r t)$	$\cos \theta$	$\sin \theta$
$\sqrt{2} S(\omega_r t) \cdot \sin(m\omega_r t)$	$J_0(\sqrt{2}\theta)$	$\sqrt{2}J_1(\sqrt{2}\theta)$

Table 1: Models for the ranging signal $r(t)$

The ranging signal $r(t)$, which is one of the four signals of Table 1, is modeled such that

$$\frac{1}{T_r} \int_0^{T_r} r^2(t) dt = 1. \quad (6)$$

So ϕ_r is the *rms* modulation index for uplink ranging.

3. UPLINK SPECTRUM

In this section, the uplink spectrum is only calculated when ranging signal alone, and no command, is present. Since the ranging signal has higher frequency content than the command signal, the effective bandwidth of the modulated uplink carrier is established reasonably well by considering only the ranging signal. A complete analysis of the uplink spectrum when both command and ranging signal are present would be considerably more involved than what appears in this paper. However, such an analysis would use the same mathematical principles outlined here.

The spectrum of the uplink carrier will change with each new step in the range code sequence. It is generally necessary to check the spectrum at each of these steps, in order to assess the interference threat.

When only ranging signal is present, the expression for uplink carrier, Eq. (1), simplifies.

$$s_u(t) = \sqrt{2} \sin[\omega_o t + \phi_r r(t)] \quad (7)$$

This can be expanded as

$$s_u(t) = \sqrt{2} \cos[\phi_r r(t)] \sin \omega_o t + \sqrt{2} \sin[\phi_r r(t)] \cos \omega_o t. \quad (8)$$

Since $r(t)$ is a periodic signal, the spectrum of this $s_u(t)$ consists only of discrete spectral lines.

The four different models for $r(t)$ are considered in separate subsections below. In each case, an expression is obtained for the power in the discrete spectral lines. For this purpose, the following definition is made.

$$\left. \frac{P_k}{P_T} \right|_{U/L} = \begin{cases} \text{fraction of uplink total power} \\ \text{in the discrete spectral line} \\ \text{with angular frequency } \omega_o + k\omega_r \end{cases}$$

In the following, $P_k/P_T|_{U/L}$ is calculated only for non-negative integers k . There is a symmetric power distribution about the carrier. So for every discrete spectral line at $\omega_o + k\omega_r$, it will be understood that there is also a discrete spectral line at $\omega_o - k\omega_r$ with the same power. $P_0/P_T|_{U/L}$ is the carrier suppression on the uplink. The conservation of energy means that

$$\left. \frac{P_0}{P_T} \right|_{U/L} + 2 \sum_{k=1}^{\infty} \left. \frac{P_k}{P_T} \right|_{U/L} = 1. \quad (9)$$

Squarewave: $r(t) = S(\omega_r t)$

The signal of Eq. (8) may be further expanded by replacing $S(\omega_r t)$ with its Fourier sine series.

$$s_u(t) = \sqrt{2} \cos \phi_r \sin \omega_o t + \sqrt{2} \sin \phi_r \sum_{\substack{k=1 \\ \text{odd}}}^{\infty} \frac{4}{\pi k} \sin(k\omega_r t) \cdot \cos \omega_o t. \quad (10)$$

The powers in the discrete spectral lines may be identified from the above as

$$\left. \frac{P_k}{P_T} \right|_{U/L} = \begin{cases} \cos^2 \phi_r, & k = 0 \\ \frac{4}{\pi^2 k^2} \sin^2 \phi_r, & k \text{ odd} \\ 0, & k \geq 2 \text{ \& even.} \end{cases} \quad (11)$$

Sinewave: $r(t) = \sqrt{2} \sin(\omega_r t)$

The signal of Eq. (8) may be expanded with the help of the Jacobi-Anger identities (Appendix A).

$$s_u(t) = \sqrt{2} J_0(\sqrt{2}\phi_r) \sin \omega_o t + 2\sqrt{2} \sum_{\substack{k=2 \\ \text{even}}}^{\infty} J_k(\sqrt{2}\phi_r) \cos(k\omega_r t) \cdot \sin \omega_o t + 2\sqrt{2} \sum_{\substack{k=1 \\ \text{odd}}}^{\infty} J_k(\sqrt{2}\phi_r) \sin(k\omega_r t) \cdot \cos \omega_o t \quad (12)$$

The function $J_k(\cdot)$ is the Bessel function of the first kind of order k . The powers in the discrete spectral lines are

$$\left. \frac{P_k}{P_T} \right|_{U/L} = J_k^2(\sqrt{2}\phi_r), \quad k \geq 0. \quad (13)$$

Squarewave Chopping: $r(t) = S(\omega_r t) \cdot S(m\omega_r t)$

The signal of Eq. (8) may be rewritten as

$$s_u(t) = \sqrt{2} \cos \phi_r \sin \omega_o t + \sqrt{2} \sin \phi_r \cdot S(\omega_r t) \cdot S(m\omega_r t) \cos \omega_o t. \quad (14)$$

$S(\omega_r t) \cdot S(m\omega_r t)$ is an even, periodic function of t . It may be written as the Fourier cosine series (Appendix B)

$$S(\omega_r t) \cdot S(m\omega_r t) = \sum_{\substack{k=1 \\ \text{odd}}}^{\infty} C_k \cos(k\omega_r t), \quad (15)$$

where

$$C_k = \frac{4 \tan\left(\frac{\pi k}{2m}\right)}{\pi k}, \quad k \text{ odd.} \quad (16)$$

The powers in the discrete spectral lines are

$$\left. \frac{P_k}{P_T} \right|_{U/L} = \begin{cases} \cos^2 \phi_r, & k = 0 \\ \frac{C_k^2}{4} \sin^2 \phi_r, & k \text{ odd} \\ 0, & k \geq 2 \text{ \& even.} \end{cases} \quad (17)$$

Sinewave Chopping: $r(t) = \sqrt{2} S(\omega_r t) \cdot \sin(m\omega_r t)$

The signal of Eq. (8) may be rewritten as

$$s_u(t) = \sqrt{2} \cos \left[\sqrt{2}\phi_r \sin(m\omega_r t) \right] \sin \omega_o t + \sqrt{2} \sin \left[\sqrt{2}\phi_r S(\omega_r t) \sin(m\omega_r t) \right] \cos \omega_o t. \quad (18)$$

$\cos[\sqrt{2}\phi_r \sin(m\omega_r t)]$ is an even, periodic function of t . It may be written as the Fourier cosine series

$$\cos[\sqrt{2}\phi_r \sin(m\omega_r t)] = J_0(\sqrt{2}\phi_r) + 2 \sum_{\substack{n=2 \\ \text{even}}}^{\infty} J_n(\sqrt{2}\phi_r) \cos(nm\omega_r t). \quad (19)$$

$\sin[\sqrt{2}\phi_r \mathcal{S}(\omega_r t) \sin(m\omega_r t)]$ is an even, periodic function of t with period T_r . It may be written as the Fourier cosine series (Appendix C)

$$\sin[\sqrt{2}\phi_r \mathcal{S}(\omega_r t) \sin(m\omega_r t)] = \sum_{\substack{k=1 \\ \text{odd}}}^{\infty} X_k \cos(k\omega_r t), \quad (20)$$

where

$$X_k = \frac{2}{\pi} \int_0^{\pi} \sin(\sqrt{2}\phi_r \sin my) \cos ky \, dy. \quad (21)$$

The integral in Eq. (21) cannot be written in terms of elementary functions; it must be evaluated numerically. The powers in the discrete spectral lines are

$$\left. \frac{P_k}{P_T} \right|_{U/L} = \begin{cases} J_n^2(\sqrt{2}\phi_r), & k = nm \ (n \geq 0 \ \& \ \text{even}) \\ \frac{X_k^2}{4}, & k \ \text{odd} \\ 0, & \text{otherwise.} \end{cases} \quad (22)$$

Comparison of Squarewave and Sinewave Chopping

Figures 2 and 3 plot $P_k/P_T|_{U/L}$ in decibels as a function of frequency for squarewave chopping and sinewave chopping, respectively. In both cases, $m = 128$ and the carrier suppression is -3.0 dB. (ϕ_r is 0.785 and 0.795 rad rms for Figures 2 and 3, respectively.) In order to better illustrate the largest harmonics, Figures 2 and 3 are magnified in Figures 4 and 5 with the horizontal axes now labeled by the harmonic number k . In both cases, the largest harmonics occur at $k = 127$ and $k = 129$. With sinewave chopping, there are also large “isolated” harmonics at $k = 256$ ($\omega_o + 2m\omega_r$) and $k = 512$ ($\omega_o + 4m\omega_r$); these are terms from Eq. (19).

In comparing Figures 2 and 3, it becomes clear why sinewave chopping is now preferred over squarewave chopping. With sinewave chopping, the power in the higher-order harmonics falls off much faster with increasing frequency. So the bandwidth of the uplink modulated carrier is significantly smaller with sinewave, rather than squarewave, chopping. From Eq. (9) and the fact that a common carrier suppression has been used, it is clear that the sum $\sum_{k=1}^{\infty} P_k/P_T$ is the same for both of these figures. In going from Figure 2 to Figure 3, a lot of high-frequency power “moves” into the isolated harmonics $k = 256$ and $k = 512$.

4. TWO-WAY PERFORMANCE

An exact analysis of two-way ranging performance would account for all command, ranging, telemetry, and noise sidebands as well as innumerable intermodulation products. Such an analysis is intractable. Approximations must be made. The approximations that are used in the two-way performance analysis of this section are summarized below.

Approximations

The function $\cos[\theta r(t)]$ is replaced by its average, which is denoted $\alpha(\theta)$,

$$\alpha(\theta) = \frac{1}{T_r} \int_0^{T_r} \cos[\theta r(t)] \, dt. \quad (23)$$

The function $\sin[\theta r(t)]$ is replaced by its lowest-order term, $\beta(\theta)r(t)$. The parameter functions $\alpha(\theta)$ and $\beta(\theta)$, which are easily evaluated using trigonometry and the Jacobi-Anger identities, are given in Table 1. When $r(t) = \pm 1$, as it does when $r(t)$ is a squarewave or a product of squarewaves, there is no error in making these replacements. In the other cases of interest, these replacements represent the approximation of ignoring all higher-order terms.

In the analysis that follows, it is necessary also to deal with functions of the form $\cos[\theta u(t)]$ and $\sin[\theta u(t)]$, where $u(t)$ is zero-mean, unity-variance, Gaussian noise and θ is a constant parameter. These functions are approximated here as (Appendix D)

$$\cos[\theta u(t)] \simeq e^{-\theta^2/2}, \quad (24)$$

and

$$\sin[\theta u(t)] \simeq \theta e^{-\theta^2/2} u(t). \quad (25)$$

The approximations of Eqs. (24) and (25) hold only for $\theta \ll 1$ rad.

Uplink

The signal model of Eq. (1) for the (unity-power) modulated uplink carrier may be expanded by means of trigonometry and the Jacobi-Anger identities. The important terms are given below. The residual carrier is

$$\sqrt{2} \alpha(\phi_r) J_0(\sqrt{2}\phi_c) \sin \omega_o t.$$

The fundamental command sidebands are given by

$$2\sqrt{2} \alpha(\phi_r) J_1(\sqrt{2}\phi_c) c(t) \sin \omega_{sc} t \cos \omega_o t.$$

The fundamental ranging sidebands are given by

$$\sqrt{2} \beta(\phi_r) J_0(\sqrt{2}\phi_c) r(t) \cos \omega_o t.$$

There are also higher-order sidebands and intermodulation products. These other terms are normally quite small. Furthermore, many of the intermodulation products are in phase quadrature to the ranging signal and so will not appear in the

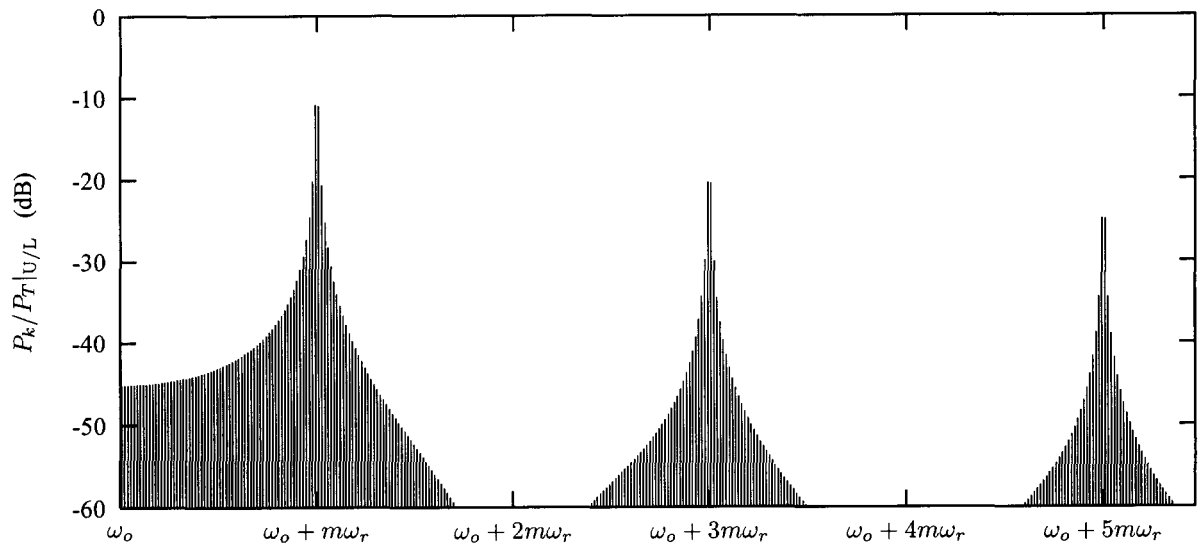


Figure 2: Uplink spectrum with *squarewave* chopping; $m = 128$, $\phi_r = 0.785$ rad

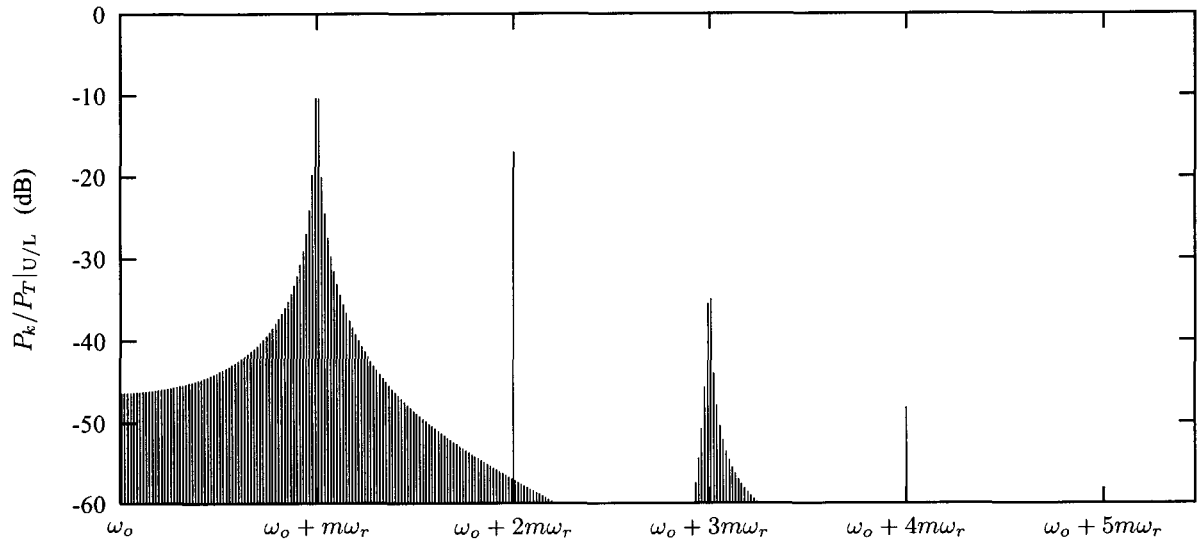


Figure 3: Uplink spectrum with *sinewave* chopping; $m = 128$, $\phi_r = 0.795$ rad

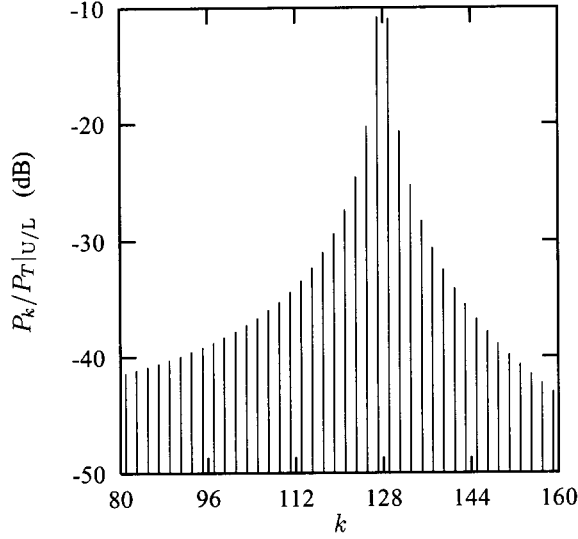


Figure 4: *Squarewave chopping*; $m = 128$, $\phi_r = 0.785$ rad

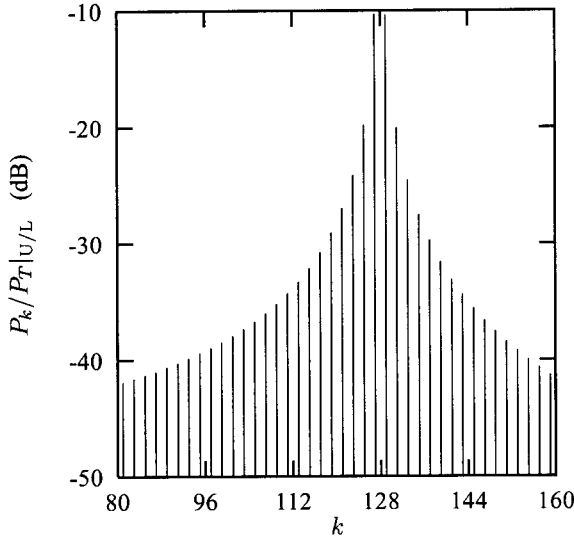


Figure 5: *Sinewave chopping*; $m = 128$, $\phi_r = 0.795$ rad

ranging channel. The higher-order terms and intermodulation products are ignored in the analysis of two-way performance appearing below.

The important power ratios for the uplink are as follows. The ratio of the residual carrier to total signal power is

$$\left. \frac{P_C}{P_T} \right|_{U/L} = \alpha^2(\phi_r) J_0^2(\sqrt{2}\phi_c). \quad (26)$$

The ratio of the ranging signal to total signal power is

$$\left. \frac{P_R}{P_T} \right|_{U/L} = \beta^2(\phi_r) J_0^2(\sqrt{2}\phi_c). \quad (27)$$

The ratio of the command (data) to total signal power is

$$\left. \frac{P_D}{P_T} \right|_{U/L} = 2\alpha^2(\phi_r) J_1^2(\sqrt{2}\phi_c). \quad (28)$$

Figure 6 diagrams the ranging channel of the spacecraft transponder. The input to the transponder ranging channel is the modulated uplink carrier that has been downconverted to an intermediate frequency. The intermediate (angular) frequency is here denoted ω_o for convenience. (Elsewhere, of course, ω_o represents the uplink carrier radio frequency.) The ranging signal is detected by multiplying the input signal by a coherent local oscillator, $\sqrt{2} \cos \omega_o t$. The post-detection filter usually has a bandwidth of 1.5 MHz so that it will pass a 1 MHz sinewave range clock. The power-controlled Automatic Gain Control (AGC) circuit adjusts the signal level so that a constant power goes to the input to the downlink phase modulator.

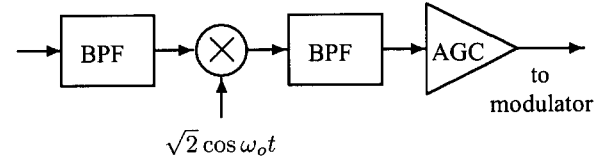


Figure 6: Spacecraft transponder ranging channel

The phase modulation of the downlink carrier due to signal plus noise in the ranging channel is

$$\psi(t) = \theta_r r(t) + \sqrt{2} \theta_c c(t) \sin \omega_{sc} t + \theta_n u(t), \quad (29)$$

where

- θ_r = downlink ranging modulation index, rad rms
- θ_c = downlink modulation index of command, rad rms
- θ_n = downlink modulation index of uplink noise, rad rms
- $u(t)$ = unity-variance, zero-mean Gaussian random process

The final term of Eq. (29) represents uplink noise in the ranging channel. The random process $u(t)$ is unity-variance, zero-mean and Gaussian with a power spectral density that is flat out to the bandwidth of the ranging channel.

Each of the modulation indices θ_r , θ_c and θ_n are in units of radians *rms*. They are given by

$$\theta_r = \theta_d \Lambda \cdot \beta(\phi_r) J_0(\sqrt{2}\phi_c), \quad (30)$$

$$\theta_c = \theta_d \Lambda \cdot \sqrt{2} \alpha(\phi_r) J_1(\sqrt{2}\phi_c), \quad (31)$$

and

$$\theta_n = \theta_d \Lambda \cdot \sigma_u. \quad (32)$$

The square of the factor σ_u is

$$\sigma_u^2 = B_R \cdot \left(\frac{P_T}{N_0} \Big|_{U/L} \right)^{-1}, \quad (33)$$

where B_R is the ranging channel bandwidth, and $P_T/N_0|_{U/L}$ is the uplink total signal power to noise spectral density ratio. The normalization factor Λ is given by

$$\Lambda = \frac{1}{\sqrt{\beta^2(\phi_r) J_0^2(\sqrt{2}\phi_c) + 2\alpha^2(\phi_r) J_1^2(\sqrt{2}\phi_c) + \sigma_u^2}}. \quad (34)$$

The downlink ranging modulation index θ_d , with units of radians *rms*, is set by the AGC circuit in the ranging channel. The average of $\psi^2(t)$ is

$$\theta_r^2 + \theta_c^2 + \theta_n^2 = \theta_d^2, \quad (35)$$

as it must be. Furthermore, the ranging signal to noise ratio is

$$\begin{aligned} \frac{\theta_r^2}{\theta_n^2} &= \frac{\beta^2(\phi_r) J_0^2(\sqrt{2}\phi_c)}{\sigma_u^2} \\ &= \frac{1}{B_R} \cdot \frac{P_R}{P_T} \Big|_{U/L} \cdot \frac{P_T}{N_0} \Big|_{U/L}, \end{aligned} \quad (36)$$

as expected.

Downlink

The modulated downlink carrier is modeled as a unity-power signal.

$$s_d(t) = \sqrt{2} \sin[G\omega_o t + \psi(t) + \theta_b b(t)] \quad (37)$$

The angular frequency of the downlink carrier is $G\omega_o$, where G is the transponding ratio. The modulating term $\psi(t)$ coming from the transponder ranging channel is given by Eq. (29). The telemetry signal $b(t) = \pm 1$ is usually either binary data on a squarewave subcarrier or just binary data. The telemetry modulation index is θ_b .

The signal model of the downlink modulated carrier may be expanded with the help of the approximations discussed previously. The most important terms are given below. The residual carrier is

$$\sqrt{2} \alpha(\theta_r) J_0(\sqrt{2}\theta_c) e^{-\theta_n^2/2} \cos(\theta_b) \sin(G\omega_o t).$$

The fundamental ranging sidebands are given by

$$\sqrt{2} \beta(\theta_r) J_0(\sqrt{2}\theta_c) e^{-\theta_n^2/2} \cos(\theta_b) r(t) \cos(G\omega_o t).$$

The telemetry sidebands are given by

$$\sqrt{2} \alpha(\theta_r) J_0(\sqrt{2}\theta_c) e^{-\theta_n^2/2} \sin(\theta_b) b(t) \cos(G\omega_o t).$$

The important power ratios for the downlink are as follows. The ratio of the residual carrier to total signal power is

$$\frac{P_C}{P_T} \Big|_{D/L} = \alpha^2(\theta_r) J_0^2(\sqrt{2}\theta_c) e^{-\theta_n^2} \cos^2(\theta_b). \quad (38)$$

The ratio of the ranging signal to total signal power is

$$\frac{P_R}{P_T} \Big|_{D/L} = \beta^2(\theta_r) J_0^2(\sqrt{2}\theta_c) e^{-\theta_n^2} \cos^2(\theta_b). \quad (39)$$

The ratio of the telemetry (data) to total signal power is

$$\frac{P_D}{P_T} \Big|_{D/L} = \alpha^2(\theta_r) J_0^2(\sqrt{2}\theta_c) e^{-\theta_n^2} \sin^2(\theta_b). \quad (40)$$

Uplink noise is also modulated onto the downlink. In general, the presence of uplink noise feeding through to the downlink has two effects on performance. First, valuable downlink power is lost in noise sidebands and noisy intermodulation products. As can be seen in Eqs. (38), (39) and (40), the result is less available power for the residual carrier, the ranging sidebands, and telemetry. Second, the uplink noise and noisy intermodulation products are themselves a source of interference. In other words, these noisy terms can, in principle, increase the effective noise floor. This effect is different in the two parallel receiver channels.

One receiver channel senses the power in the residual carrier. When the downlink signal $s_d(t)$ is of the form given by Eq. (37), this channel uses a local oscillator $\sin(G\omega_o t)$ for detection of the residual carrier. This channel is called the *in-phase* channel because the local oscillator is in-phase with the residual carrier. The intermodulation product of uplink noise with telemetry is on this channel; it is of the form

$$-\sqrt{2} \alpha(\theta_r) J_0(\sqrt{2}\theta_c) \theta_n e^{-\theta_n^2/2} \sin(\theta_b) u(t) b(t) \sin(G\omega_o t).$$

The power of this intermodulation product, as a fraction of the total downlink signal power, is given by

$$\frac{P_{NI}}{P_T} \Big|_{D/L} = \alpha^2(\theta_r) J_0^2(\sqrt{2}\theta_c) \theta_n^2 e^{-\theta_n^2} \sin^2(\theta_b). \quad (41)$$

The subscript ‘‘NI’’ refers to noisy sidebands on the in-phase channel. The approximation is made here that this noise power is spread evenly over the bandwidth B_R . This is not an unreasonable approximation if the telemetry subcarrier has a frequency that is small compared with B_R . (If the telemetry subcarrier is *not* small compared with B_R , the approximation is still useful, as it leads to a worst-case bound on performance.) With this approximation, the downlink noise floor on the in-phase channel is increased by a factor

$$\Gamma_I = 1 + \frac{1}{B_R} \cdot \frac{P_T}{N_0} \Big|_{D/L} \cdot \frac{P_{NI}}{P_T} \Big|_{D/L}. \quad (42)$$

This elevated noise floor on the in-phase channel can affect conical-scan (conscan) pointing of the earth antenna. This problem is discussed in Section 5.

The other receiver channel demodulates telemetry and ranging signals. When the downlink signal $s_d(t)$ is of the form given by Eq. (37), this channel uses a local oscillator $\cos(G\omega_o t)$ for detection of telemetry and ranging. This channel is called the *quadrature* channel because the local oscillator and residual carrier are out of phase by a quarter cycle. The uplink noise plus some intermodulation products involving noise are on this channel. This noisy quadrature-channel power, as a fraction of the total downlink signal power, may be approximated by

$$\begin{aligned} \frac{P_{NQ}}{P_T} \Big|_{D/L} &= \theta_n^2 e^{-\theta_n^2} \times \\ &\left[\alpha^2(\theta_r) J_0^2(\sqrt{2}\theta_c) \cos^2(\theta_b) \right. \\ &+ 2\beta(\theta_r) J_0^2(\sqrt{2}\theta_c) \sin^2(\theta_b) \\ &\left. + 2\alpha^2(\theta_r) J_1^2(\sqrt{2}\theta_c) \sin^2(\theta_b) \right]. \end{aligned} \quad (43)$$

The subscript “NQ” refers to noisy sidebands on the quadrature channel. The first of the three terms in the bracket of Eq. (43) represents uplink noise sidebands. The second term represents the intermodulation product of uplink noise with ranging and telemetry sidebands. The third term represents the intermodulation product of uplink noise with command and telemetry sidebands. (There are other noisy intermodulation products, but they are typically small by comparison.) As with the in-phase channel, the approximation is made that this noise power is spread evenly over the bandwidth B_R . While not really true, this approximation leads to a simple, worst-case model. With this approximation, the downlink noise floor on the quadrature channel is increased by a factor

$$\Gamma_Q = 1 + \frac{1}{B_R} \cdot \frac{P_T}{N_0} \Big|_{D/L} \cdot \frac{P_{NQ}}{P_T} \Big|_{D/L}. \quad (44)$$

This factor is plotted in Figure 7 as a function of $P_T/N_0|_{D/L}$ assuming uplink noise alone is in the transponder ranging channel (as happens when the ranging channel is “on” but the ranging signal has not yet arrived). Here $\theta_n = \theta_d$, and $\theta_r = \theta_c = 0$. The telemetry modulation index is taken to be 45° , and B_R is 1.5 MHz. The factor Γ_Q is plotted for two different values of θ_d .

The general equations governing the distribution of power in the downlink are Eqs. (38), (39) and (40). In a typical deep space scenario, the uplink noise dominates the ranging channel, so that $\theta_n \simeq \theta_d$ and $\theta_c \ll \theta_d$. Since the Bessel function $J_0(\cdot)$ equals approximately 1 for small values of its argument, the Bessel functions of Eqs. (38), (39) and (40) are typically ignored. In other words, in a typical deep space scenario the command signal that feeds through the ranging channel has no significant effect on telemetry or two-way ranging performance. It is important to note here,

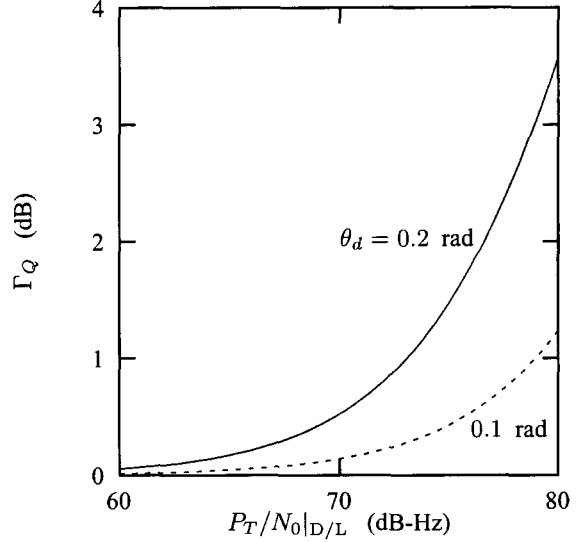


Figure 7: Factor Γ_Q ; $B_R = 1.5$ MHz, $\theta_b = 45^\circ$

however, that in the early mission phase, where ranging and command signal, rather than uplink noise, generally dominate the ranging channel, the effect of command signal feeding through to the downlink must be taken into account in order to predict with accuracy the performance of both telemetry and two-way ranging.

Range Measurement Error

Downlink noise causes an error in the two-way range measurement. This is not the only error in range measurement, but it is an important error. A relatively simple theory exists for predicting this error, as seen below, and so this error can be controlled with the selection of appropriate integration times. The derivation of the range measurement error due to downlink noise has appeared elsewhere, for example in Reference [4]. A terse restatement of this derivation appears below.

Here it is assumed that the range clock is a sinewave. This is usually the case.

$$r(t) = \sqrt{2} \sin \omega_r t \quad (45)$$

This range clock appears in the demodulator output of the ground receiver. It is accompanied by additive, white, Gaussian noise, which is here denoted $n(t)$. The range clock is modeled with unity power, as seen in Eq. (45), so in order to maintain the correct signal-to-noise spectral density ratio, the downlink noise $n(t)$ must be modeled with a one-sided power spectral density of

$$\left(\frac{P_R}{N_0} \Big|_{D/L} \right)^{-1},$$

where

$$\frac{P_R}{N_0} \Big|_{D/L} = \frac{P_R}{P_T} \Big|_{D/L} \cdot \frac{P_T}{N_0} \Big|_{D/L} \quad (46)$$

The ratio $P_R/P_T|_{D/L}$ is given by Eq. (39). $P_T/N_0|_{D/L}$ is the total downlink signal power to noise spectral density ratio.

The arriving range clock is subjected to two correlations occurring in parallel. The integration time of each correlation is T_1 . In this analysis, T_1 is taken to be

$$T_1 = KT_r, \quad (47)$$

where K is an integer and T_r her e denotes the period of the range clock. It is not necessary that T_1 be an integer multiple of T_r . It is only that this analysis is simplified and no significant loss of precision occurs if the final $T_1 \bmod T_r$ of the integration is ignored. One correlation uses a reference squarewave having the same frequency as $r(t)$. This correlation gives

$$x = \frac{1}{T_1} \sum_{k=0}^{K-1} \int_{kT_r}^{(k+\frac{1}{2})T_r} [r(t-\tau) + n(t)] dt - \frac{1}{T_1} \sum_{k=0}^{K-1} \int_{(k+\frac{1}{2})T_r}^{(k+1)T_r} [r(t-\tau) + n(t)] dt, \quad (48)$$

where τ is the two-way delay. The other correlation uses a reference squarewave that equals the previous reference squarewave delayed by a quarter cycle. This other correlation gives

$$y = \frac{1}{T_1} \sum_{k=0}^{K-1} \int_{(k+\frac{1}{4})T_r}^{(k+\frac{3}{4})T_r} [r(t-\tau) + n(t)] dt - \frac{1}{T_1} \sum_{k=0}^{K-1} \int_{(k+\frac{3}{4})T_r}^{(k+\frac{1}{2})T_r} [r(t-\tau) + n(t)] dt. \quad (49)$$

In the absence of noise, x is

$$\bar{x} = \frac{2\sqrt{2}}{\pi} \cos \omega_r \tau \quad (50)$$

and y is

$$\bar{y} = \frac{2\sqrt{2}}{\pi} \sin \omega_r \tau. \quad (51)$$

Downlink noise contributes a variance to these correlation values.

$$\sigma_x^2 = \sigma_y^2 = \frac{1}{2T_1} \cdot \left(\frac{P_R}{N_0} \Big|_{D/L} \right)^{-1} \quad (52)$$

The two-way delay, when measured in units of T_r , has a fractional part that can be estimated from x and y . This estimated (fractional) delay is

$$\hat{\tau} = \frac{1}{\omega_r} \tan^{-1} \left(\frac{y}{x} \right). \quad (53)$$

The variance on this measurement may be approximated by

$$\sigma_{\hat{\tau}}^2 = \sigma_x^2 \left[\frac{\partial \hat{\tau}}{\partial x} \Big|_{(\bar{x}, \bar{y})} \right]^2 + \sigma_y^2 \left[\frac{\partial \hat{\tau}}{\partial y} \Big|_{(\bar{x}, \bar{y})} \right]^2, \quad (54)$$

which can be written as

$$\sigma_{\hat{\tau}}^2 = \left[64 T_1 f_r^2 \cdot \frac{P_R}{N_0} \Big|_{D/L} \right]^{-1}, \quad (55)$$

where $f_r = \omega_r/(2\pi)$ is the cyclical frequency of the range clock. The variance $\sigma_{\hat{\rho}}^2$ of the range measurement, in distance units squared, is given by

$$\begin{aligned} \sigma_{\hat{\rho}}^2 &= \left(\frac{c}{2} \right)^2 \sigma_{\hat{\tau}}^2 \\ &= c^2 \left[256 T_1 f_r^2 \cdot \frac{P_R}{N_0} \Big|_{D/L} \right]^{-1}. \end{aligned} \quad (56)$$

It is important to remember that $\hat{\tau}$ is a measure of the *fractional* part of the two-way delay. That is to say, in the absence of measurement error,

$$\hat{\tau} = \tau \bmod T_r. \quad (57)$$

The *integer* part of the two-way delay ($\tau - \tau \bmod T_r$), an integer multiple of T_r , is determined by use of the ambiguity-resolving components plus the *a priori* knowledge of the range. The use of the ambiguity-resolving components is discussed in the next subsection.

The astute reader may suspect that a better measurement of τ in the presence of noise could be made if reference *sinewaves* are used instead of reference *squarewaves*. This is perfectly true. If reference sinewaves were used, the error variances of Eqs. (55) and (56) would be smaller by a factor $8/\pi^2$. That is to say, with reference sinewaves the signal-to-noise ratio could be smaller by 0.9 dB and still achieve the same measurement error due to noise. The initial implementation of the range measurement signal processing uses the correlations of Eqs. (48) and (49). It would take a future enhancement of the signal processing, permitting sinewave correlations, to achieve the 0.9 dB improvement discussed in this paragraph.

Probability of Acquisition

The range measurement is not yet finished. There is ambiguity in the measured delay of a periodic signal. The set of all two-way delays that are consistent with the range measurement just made would look, if marked on a horizontal time axis, like a "comb" of uniformly spaced permissible values. The spacing between any two adjacent permissible values would equal the period of the range clock. The ambiguity is gradually resolved by a sequence of correlations against the ambiguity-resolving components (that is, all components following the range clock). But before these correlations are performed, the relative delay of the received ranging signal is reduced by $\hat{\tau}$. (This is implemented by delaying the reference squarewaves by $\hat{\tau}$.) After this adjustment, the new relative delay ($\tau - \hat{\tau}$) is (approximately) an integer multiple of the period of the range clock. The integration time for each of the ambiguity-resolving correlations is T_2 .

In the discussion that follows, the parameter T_c represents the period of the *current* component. As the second component arrives, its period T_c is twice that of the range clock. The integration time T_2 is taken to be

$$T_2 = K'T_c, \quad (58)$$

where K' is an integer. The fractional part of T_2 , when measured in units of T_c , can be safely ignored. The correlation against this component gives

$$x = \frac{1}{T_2} \sum_{k=0}^{K'-1} \int_{kT_c}^{(k+\frac{1}{2})T_c} [r(t - \tau') + n(t)] dt - \frac{1}{T_2} \sum_{k=0}^{K'-1} \int_{(k+\frac{1}{2})T_c}^{(k+1)T_c} [r(t - \tau') + n(t)] dt, \quad (59)$$

where the new relative delay $\tau' = \tau - \hat{\tau}$ is an integer M multiple of the range clock period. In the absence of noise, the value of this correlation has one of two values. If the component is a squarewave or a squarewave chopped by a squarewave, the noiseless correlation is either $+1$ (for an even M) or -1 (for an odd M). If the component is a sine wave or a squarewave chopped by a sine wave, the noiseless correlation is either $+2\sqrt{2}/\pi$ (for an even M) or $-2\sqrt{2}/\pi$ (for an odd M).

If the correlation value is negative, the relative delay is further reduced by an amount $T_c/2$. If the correlation value is positive, no correction is made. This has the effect of ensuring that the adjusted relative delay is an integer multiple of the second component. Thus, the spacing between adjacent possibilities in the “comb” of permissible delays has been doubled. (The spacing had been the range clock period, and now it is twice that.)

In this way, correlation is made against one component after another. At the end of the sequence, the spacing between adjacent possibilities in the “comb” of permissible delays is 2^{n-1} times the range clock period, where n is the number of components in the sequence. Presumably, n has been chosen large enough that this spacing is larger than the uncertainty in the *a priori* estimate of the two-way delay. A final determination of the two-way delay takes account of the delay corrections made for each negative correlation as well as the initial measured value of $\hat{\tau}$.

It is important to consider the effect of downlink noise on this decision process. With each correlation there is a risk that a -1 or $-2\sqrt{2}/\pi$ will appear positive in the presence of downlink noise. Also, a $+1$ or $+2\sqrt{2}/\pi$ may appear negative. The downlink noise contributes a variance σ_x^2 to the correlation.

$$\sigma_x^2 = \frac{1}{2T_2} \cdot \left(\frac{P_R}{N_0} \Big|_{D/L} \right)^{-1} \quad (60)$$

If the component is a squarewave or a squarewave chopped by a squarewave, the probability of correctly identifying the sign

of the correlation is

$$\frac{1}{\sqrt{2\pi\sigma_x^2}} \int_{-1}^{\infty} \exp\left(\frac{-x^2}{2\sigma_x^2}\right) dx = \frac{1}{2} + \frac{1}{2} \operatorname{erf}\left(\sqrt{T_2 \cdot \frac{P_R}{N_0}} \Big|_{D/L}\right). \quad (61)$$

Similarly, if the component is a sine wave or a squarewave chopped by a sine wave, the probability of correctly identifying the sign of the correlation is

$$\frac{1}{\sqrt{2\pi\sigma_x^2}} \int_{-2\sqrt{2}/\pi}^{\infty} \exp\left(\frac{-x^2}{2\sigma_x^2}\right) dx = \frac{1}{2} + \frac{1}{2} \operatorname{erf}\left(\sqrt{\frac{8}{\pi^2} T_2 \cdot \frac{P_R}{N_0}} \Big|_{D/L}\right). \quad (62)$$

The abbreviation $\operatorname{erf}(\cdot)$ is used for the error function,

$$\operatorname{erf}(y) = \frac{2}{\sqrt{\pi}} \int_0^y \exp(-t^2) dt. \quad (63)$$

A legitimate range measurement occurs only when the signs of all ambiguity-resolving component correlations are correctly identified. Denoting the probability of correct identification for the i th component by p_i , where $i = 2, 3, \dots, n$, the probability of acquisition of the ranging sequence is

$$\text{Probability of Acquisition} = \prod_{i=2}^n p_i, \quad (64)$$

where n is the number of components in the sequence. Each p_i in Eq. (64) is one of the expressions Eq. (61) or (62). If, at some future date, correlation with sine wave references is made available in the range measurement signal processing, then Eq. (61) would apply to all components.

5. CONSCAN PROBLEM

The conscan technique is used for closed-loop pointing of earth station antennas toward deep space vehicles.[5] When conscan is active, the antenna boresight is intentionally scanned in a repetitive, conical pattern in order to induce small changes in the received residual-carrier power. From these changes, an angular error signal may be derived. This error signal is the feedback signal that makes closed-loop control possible. For conscan to work well, an accurate measure of the time variation of the residual-carrier power is required. Since carrier power is a function of receiving system gain, which varies whenever gain is under automatic control, the receiver instead estimates the ratio of residual-carrier power to noise spectral density, which is independent of system gain. Abrupt changes in this estimated ratio are interpreted by the control algorithm as angular pointing errors. Therefore, an artificial and abrupt change in the estimated ratio that occurs in the absence of a pointing offset will confuse the conscan algorithm. It has been observed

that this sometimes occurs during early mission phase in the presence of a ranging signal. In the following paragraphs, an analytical explanation is offered for this phenomenon.

As described in Section 4, there is an intermodulation product of uplink noise with telemetry that can increase the effective noise floor on the in-phase downlink channel. The factor by which the effective noise floor is increased is Γ_I , and it is given by Eq. (42). The effective value for the ratio of residual-carrier power to noise spectral density is

$$\frac{P_C}{N_0}|_{\text{eff}} = \frac{P_C}{P_T}|_{\text{D/L}} \cdot \frac{P_T}{N_0}|_{\text{D/L}} \cdot \Gamma_I^{-1}. \quad (65)$$

The problem is that $P_C/N_0|_{\text{eff}}$ can change significantly during the ranging sequence, even in the absence of a pointing offset.

During early mission phase, with the transponder ranging channel “on” but before the first ranging component appears (and assuming no command), only uplink noise is present in the ranging channel. The ranging channel AGC amplifies this uplink noise with relatively large gain and then passes this amplified noise along to the downlink modulator. When the first ranging component arrives, the ranging channel AGC gain decreases dramatically from what it had just been, assuming the ranging channel signal-to-noise ratio is large (as it often is during early mission phase). Now there is essentially no noise (but plenty of ranging signal) modulated onto the downlink. The intermodulation products of uplink noise with telemetry now disappear. If $P_T/N_0|_{\text{D/L}}$ is large, the effective noise floor suddenly decreases significantly. This means an abrupt change in $P_C/N_0|_{\text{eff}}$. (At the end of the ranging sequence, when the last ranging component departs, there is another abrupt change in $P_C/N_0|_{\text{eff}}$.) In Eq. (65), it is the factor Γ_I that changes dramatically. ($P_C/P_T|_{\text{D/L}}$ also changes, but this is a small effect.) It is of interest to calculate the factor by which $P_C/N_0|_{\text{eff}}$ changes as the first ranging component arrives. This factor is given by

$$1 + \frac{1}{B_R} \cdot \frac{P_T}{N_0}|_{\text{D/L}} \cdot \theta_d^2 e^{-\theta_d^2} \sin^2(\theta_b). \quad (66)$$

This factor is plotted in Figure 8 as a function of $P_T/N_0|_{\text{D/L}}$ for a telemetry modulation index of 80 and for $B_R = 1.5$ MHz. Two different values of θ_d are shown. For a sufficiently large $P_T/N_0|_{\text{D/L}}$, the abrupt change in $P_C/N_0|_{\text{eff}}$ is large enough to foil conscan pointing. This has been observed in practice.

6. CONCLUSIONS

This paper analyzes both the uplink spectrum and the two-way performance of sequential ranging with the new signal structure specified by the Network Simplification Plan, which calls for sinewaves to replace squarewaves for the highest-frequency components. The spectrum of the uplink carrier is considerably narrowed by the change to sinewaves.

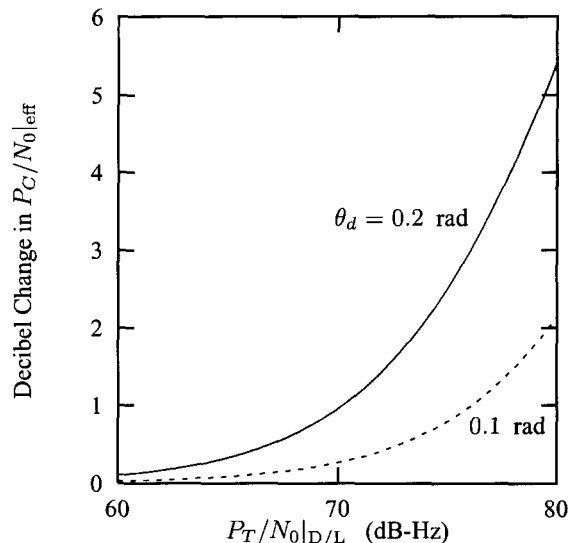


Figure 8: Change in $P_C/N_0|_{\text{eff}}$; $B_R = 1.5$ MHz, $\theta_b = 80^\circ$

A general analysis of two-way performance in the presence of noise is also given. The feeding through of command signals onto the downlink is incorporated in the analysis because this can be significant during early mission phase. Finally, an explanation is given for the observed problem of conscan tracking during sequential ranging measurements in early mission phase.

APPENDIX A: JACOBI-ANGER IDENTITIES

The expression

$$\cos(y \sin x)$$

is an even, periodic function of x . It may therefore be expanded in a Fourier cosine series. The coefficients are Bessel functions of the first kind.

$$\cos(y \sin x) = J_0(y) + 2 \sum_{\substack{k=2 \\ \text{even}}}^{\infty} J_k(y) \cos(kx) \quad (\text{A-1})$$

The expression

$$\sin(y \sin x)$$

is an odd, periodic function of x . It may be expanded in a Fourier sine series.

$$\sin(y \sin x) = 2 \sum_{\substack{k=1 \\ \text{odd}}}^{\infty} J_k(y) \sin(kx) \quad (\text{A-2})$$

These are the Jacobi-Anger identities.

APPENDIX B: SQUAREWAVE CHOPPING

In this appendix, a Fourier series representation is found for

$$r(t) = S(\omega_r t) \cdot S(m\omega_r t), \quad (\text{B-1})$$

where m is a power of 2. The period of $r(t)$ is $T_r = 2\pi/\omega_r$, and $r(t)$ may be written as the Fourier series

$$r(t) = \sum_{k=-\infty}^{\infty} \frac{C_k}{2} e^{j2\pi kt/T_r}, \quad (\text{B-2})$$

where

$$C_k = \frac{2}{T_r} \int_0^{T_r} r(t) e^{-j2\pi kt/T_r} dt. \quad (\text{B-3})$$

As shown below, some of the Fourier series coefficients vanish. For example, $C_0 = 0$ since $r(t)$ has zero average.

The integral of Eq. (B-3) is broken into two smaller integrals. The first, from 0 to $T_r/2$, is further divided into m integrals, each corresponding to one horizontal line segment of $r(t)$. The second, from $T_r/2$ to T_r , is also divided into m integrals. Eq. (B-3) then becomes

$$C_k = U_1 - U_2, \quad (\text{B-4})$$

where

$$U_1 = \frac{2}{T_r} \sum_{n=0}^{m-1} (-1)^n \int_{\frac{nT_r}{2m}}^{\frac{(n+1)T_r}{2m}} e^{-j2\pi kt/T_r} dt, \quad (\text{B-5})$$

and

$$U_2 = \frac{2}{T_r} \sum_{n=m}^{2m-1} (-1)^n \int_{\frac{nT_r}{2m}}^{\frac{(n+1)T_r}{2m}} e^{-j2\pi kt/T_r} dt. \quad (\text{B-6})$$

U_2 may be put into a form like that of U_1 with the two substitutions $n' = n - m$ and $t' = t - \frac{T_r}{2}$. Eq. (B-6) then becomes

$$U_2 = e^{-j\pi k} U_1. \quad (\text{B-7})$$

Combining Eqs. (B-4) and (B-7) gives

$$C_k = (1 - e^{-j\pi k}) U_1. \quad (\text{B-8})$$

The Fourier coefficients vanish for even values of k ,

$$C_k = 0, \quad k \text{ even}. \quad (\text{B-9})$$

It remains to determine the Fourier coefficients for odd values of k .

$$C_k = 2U_1, \quad k \text{ odd} \quad (\text{B-10})$$

The integral in Eq. (B-5) is easily evaluated.

$$\int_{\frac{nT_r}{2m}}^{\frac{(n+1)T_r}{2m}} e^{-j2\pi kt/T_r} dt = \frac{T_r \sin\left(\frac{\pi k}{2m}\right) \exp\left(-j\frac{\pi k}{2m}\right)}{\pi k} e^{-j\pi kn/m} \quad (\text{B-11})$$

Combining Eqs. (B-5), (B-10) and (B-11) gives

$$C_k = \frac{4 \sin\left(\frac{\pi k}{2m}\right) \exp\left(-j\frac{\pi k}{2m}\right)}{\pi k} \times \sum_{n=0}^{m-1} \left(-e^{-j\pi k/m}\right)^n, \quad k \text{ odd}. \quad (\text{B-12})$$

The sum in Eq. (B-12) can be evaluated with the help of the identity

$$\sum_{n=0}^{m-1} y^n = \frac{y^m - 1}{y - 1}. \quad (\text{B-13})$$

The substitution of $y = -e^{-j\pi k/m}$ into Eq. (B-13) gives

$$\sum_{n=0}^{m-1} \left(-e^{-j\pi k/m}\right)^n = \frac{1 - e^{-j\pi k}}{1 + e^{-j\pi k/m}}. \quad (\text{B-14})$$

For odd values of k , Eq. (B-14) becomes

$$\sum_{n=0}^{m-1} \left(-e^{-j\pi k/m}\right)^n = \frac{\exp\left(\frac{j\pi k}{2m}\right)}{\cos\left(\frac{\pi k}{2m}\right)}, \quad k \text{ odd}. \quad (\text{B-15})$$

Combining Eqs. (B-12) and (B-15) gives

$$C_k = \frac{4 \tan\left(\frac{\pi k}{2m}\right)}{\pi k}, \quad k \text{ odd}. \quad (\text{B-16})$$

From Eqs. (B-9) and (B-16) it is clear that

$$C_{-k} = C_k. \quad (\text{B-17})$$

Therefore the Fourier series of Eq. (B-2) may be rewritten as the Fourier cosine series

$$r(t) = \sum_{\substack{k=1 \\ \text{odd}}}^{\infty} C_k \cos(2\pi kt/T_r), \quad (\text{B-18})$$

where the coefficients are given by Eq. (B-16). It is natural that this $r(t)$ can be represented by a Fourier cosine series, since it possesses even symmetry.

APPENDIX C: SINEWAVE CHOPPING

In this appendix, a Fourier series representation is found for

$$x(t) = \sin\left[\sqrt{2}\phi_r S(\omega_r t) \sin(m\omega_r t)\right], \quad (\text{C-1})$$

where m is a power of 2. $x(t)$ is an even, periodic function of t with period $T_r = 2\pi/\omega_r$; it may be represented by the Fourier cosine series

$$x(t) = \sum_{k=0}^{\infty} X_k \cos(k\omega_r t), \quad (\text{C-2})$$

where

$$X_k = \frac{2}{T_r} \int_0^{T_r} x(t) \cos(k\omega_r t) dt. \quad (\text{C-3})$$

As shown below, some of the Fourier series coefficients vanish. For example, $X_0 = 0$ since the signal average is zero.

The integral of Eq. (C-3) is broken into two parts.

$$X_k = V_1 - V_2, \quad (\text{C-4})$$

where

$$V_1 = \frac{2}{T_r} \int_0^{\frac{T_r}{2}} \sin \left[\sqrt{2} \phi_r \sin(m\omega_r t) \right] \cos(k\omega_r t) dt, \quad (\text{C-5})$$

and

$$V_2 = \frac{2}{T_r} \int_{\frac{T_r}{2}}^{T_r} \sin \left[\sqrt{2} \phi_r \sin(m\omega_r t) \right] \cos(k\omega_r t) dt \quad (\text{C-6})$$

V_2 may be put into a form like that of V_1 with the substitution $t' = t - \frac{T_r}{2}$. Eq. (C-6) then becomes

$$V_2 = \begin{cases} -V_1, & k \text{ odd} \\ V_1, & k \text{ even.} \end{cases} \quad (\text{C-7})$$

Combining Eqs. (C-4) and (C-7) gives

$$X_k = \begin{cases} 2V_1, & k \text{ odd} \\ 0, & k \text{ even.} \end{cases} \quad (\text{C-8})$$

When Eqs. (C-5) and (C-8) are combined and a simple change is made in the variable of integration, a convenient expression is obtained.

$$X_k = \frac{2}{\pi} \int_0^{\pi} \sin \left(\sqrt{2} \phi_r \sin my \right) \cos ky dy, \quad k \text{ odd} \quad (\text{C-9})$$

Since the Fourier coefficients vanish for even k , the Fourier cosine series may be written as

$$x(t) = \sum_{\substack{k=1 \\ \text{odd}}}^{\infty} X_k \cos(k\omega_r t). \quad (\text{C-10})$$

APPENDIX D: NOISE APPROXIMATIONS

Unity-variance, zero-mean, Gaussian noise $u(t)$ appears in the following two functions: $\cos[\theta u(t)]$ and $\sin[\theta u(t)]$. A lowest-order approximation is used for each. First, $\cos[\theta u(t)]$ is approximated by its mean

$$\cos[\theta u(t)] \simeq \gamma(\theta), \quad (\text{D-1})$$

where

$$\gamma(\theta) = \frac{1}{\sqrt{2\pi}} \int_{-\infty}^{\infty} \cos(\theta u) e^{-u^2/2} du. \quad (\text{D-2})$$

It is noted that

$$\gamma(0) = 1. \quad (\text{D-3})$$

Differentiating Eq. (D-2) with respect to θ gives

$$\frac{d\gamma(\theta)}{d\theta} = \frac{1}{\sqrt{2\pi}} \int_{-\infty}^{\infty} \sin(\theta u) \left[-ue^{-u^2/2} \right] du. \quad (\text{D-4})$$

Integrating Eq. (D-4) by parts gives

$$\begin{aligned} \frac{d\gamma(\theta)}{d\theta} &= -\theta \cdot \frac{1}{\sqrt{2\pi}} \int_{-\infty}^{\infty} \cos(\theta u) e^{-u^2/2} du \\ &= -\theta \cdot \gamma(\theta). \end{aligned} \quad (\text{D-5})$$

Combining this differential equation with the constraint of Eq. (D-3) leads to the unique solution

$$\gamma(\theta) = e^{-\theta^2/2}. \quad (\text{D-6})$$

The function $\sin[\theta u(t)]$, which has zero mean, is approximated as

$$\sin[\theta u(t)] \simeq \theta \gamma(\theta) u(t). \quad (\text{D-7})$$

This approximation is justified by two observations. First, the expected value of both sides of Eq. (D-7) is 0. Second, multiplying one side of Eq. (D-7) by $u(t)$ and then taking the expectation gives the same result as multiplying the other side by $u(t)$ and then taking the expectation. That is,

$$E\{u \sin(\theta u)\} = E\{\theta \gamma(\theta) u^2\}. \quad (\text{D-8})$$

This second observation is now demonstrated.

$$E\{u \sin(\theta u)\} = \frac{1}{\sqrt{2\pi}} \int_{-\infty}^{\infty} u \sin(\theta u) e^{-u^2/2} du \quad (\text{D-9})$$

Integrating by parts yields

$$\begin{aligned} E\{u \sin(\theta u)\} &= \theta \cdot \frac{1}{\sqrt{2\pi}} \int_{-\infty}^{\infty} \cos(\theta u) e^{-u^2/2} du \\ &= \theta \cdot \gamma(\theta). \end{aligned} \quad (\text{D-10})$$

Also,

$$\begin{aligned} E\{\theta \gamma(\theta) u^2\} &= \theta \gamma(\theta) E\{u^2\} \\ &= \theta \gamma(\theta). \end{aligned} \quad (\text{D-11})$$

A comparison of Eqs. (D-10) and (D-11) confirms that Eq. (D-8) is true.

ACKNOWLEDGMENT

The research described in this paper was carried out at the Jet Propulsion Laboratory, California Institute of Technology, under a contract with the National Aeronautics and Space Administration.